Human Reproduction, Vol.24, No.7 pp. 1704–1716, 2009
Advanced Access publication on March 31, 2009 doi:10.1093/humrep/dep073

human reproduction

ORIGINAL ARTICLE *Reproductive biology*

Molecular dissection of the male germ cell lineage identifies putative spermatogonial stem cells in rhesus macaques

Brian P. Hermann[1,4,5], Meena Sukhwani[5], David R. Simorangkir[2,4,5], Tianjiao Chu[1,5], Tony M. Plant[2,4,5], and Kyle E. Orwig[1,3,4,5,6]

[1]Department of Obstetrics, Gynecology and Reproductive Sciences, University of Pittsburgh School of Medicine, Pittsburgh, PA 15260, USA [2]Department of Cell Biology and Physiology, University of Pittsburgh School of Medicine, Pittsburgh, PA 15260, USA [3]Department of Microbiology and Molecular Genetics, University of Pittsburgh School of Medicine, Pittsburgh, PA 15260, USA [4]Center for Research in Reproductive Physiology, University of Pittsburgh School of Medicine, Pittsburgh, PA 15260, USA [5]Magee-Womens Research Institute, Pittsburgh, PA 15213, USA

[6]Correspondence address. Magee-Womens Research Institute, 204 Craft Avenue, Room B711, Pittsburgh, PA 15213 USA; Tel: +1-412-641-2460; Fax: +1-412-641-3899; E-mail: orwigke@upmc.edu

BACKGROUND: The spermatogonial stem cell (SSC) pool in the testes of non-human primates is poorly defined.

METHODS: To begin characterizing SSCs in rhesus macaque testes, we employed fluorescence-activated cell sorting (FACS), a xenotransplant bioassay and immunohistochemical methods and correlated our findings with classical descriptions of germ cell nuclear morphology (i.e. A_{dark} and A_{pale} spermatogonia).

RESULTS: FACS analysis identified a THY-1$^+$ fraction of rhesus testis cells that was enriched for consensus SSC markers (i.e. PLZF, GFRα1) and exhibited enhanced colonizing activity upon transplantation to nude mouse testes. We observed a substantial conservation of spermatogonial markers from mice to monkeys [PLZF, GFRα1, Neurogenin 3 (NGN3), cKIT]. Assuming that molecular characteristics correlate with function, the pool of putative SSCs (THY-1$^+$, PLZF$^+$, GFRα1$^+$, NGN3$^{+/-}$, cKIT$^-$) comprises most A_{dark} and A_{pale} and is considerably larger in primates than in rodents. It is noteworthy that the majority of A_{dark} and A_{pale} share a common molecular phenotype, considering their distinct functional classifications as reserve and renewing stem cells, respectively. NGN3 is absent from A_{dark}, but is expressed by some A_{pale} and may mark the transition from undifferentiated (cKIT$^-$) to differentiating (cKIT$^+$) spermatogonia. Finally, the pool of transit-amplifying progenitor spermatogonia (PLZF$^+$, GFRα1$^+$, NGN3$^+$, cKIT$^{+/-}$) is smaller in primates than in rodents.

CONCLUSIONS: These results provide an in-depth analysis of molecular characteristics of primate spermatogonia, including SSCs, and lay a foundation for future studies investigating the kinetics of spermatogonial renewal, clonal expansion and differentiation during primate spermatogenesis.

Key words: spermatogonial stem cells / A_{dark} spermatogonia / A_{pale} spermatogonia / xenotransplantation / primate

Introduction

Spermatogonial stem cells (SSCs) are undifferentiated germ cells that balance self-renewing and differentiating divisions to maintain spermatogenesis throughout adult life. Investigating the biological properties of SSCs may provide general insights for understanding stem cell biology and tissue development. Furthermore, the regenerative potential of SSCs has been exploited in a transplantation paradigm to restore spermatogenesis in infertile animal models [rodents (Ogawa *et al.*, 2000; Nagano *et al.*, 2001; Brinster *et al.*, 2003; Ryu *et al.*, 2003),

goats (Honaramooz *et al*., 2003) and dogs (Kim *et al*., 2008)]. This stem cell therapy may one day have application for treating some cases of human male infertility (reviewed in Orwig and Schlatt, 2005; Brinster, 2007; Geens *et al*., 2008). Elucidating fundamental characteristics of the SSC pool in a non-human primate model may facilitate translation of SSC transplantation to the clinic. Although the cellular and molecular characteristics of SSCs remain elusive, particularly in primates, insights can be gleaned from progress studying rodent SSCs.

Rodent SSCs can be identified in whole-mount preparations of testicular seminiferous tubules [initially described by Clermont and Bustos-Obregon (1968)] as isolated A_{single} spermatogonia. In addition to $A_{singles}$, the rodent SSC pool must also include some A_{paired} spermatogonia that will complete cytokinesis to maintain the pool of $A_{singles}$. These SSCs are present on the basement membrane of seminiferous tubules and can be distinguished from committed, transit-amplifying progenitor spermatogonia on the basis of clone size ($A_{aligned}$ spermatogonia exist as chains of 4–16 cells connected by intercellular cytoplasmic bridges). Here we define progenitors as undifferentiated spermatogonia that are committed to differentiate, but can undergo a finite number of self-renewing divisions. Although no SSC-specific marker has been identified, whole-mount analyses indicate that GFRα1, PLZF, CDH1 and OCT3/4 are expressed by undifferentiated spermatogonia, including A_{single}, A_{paired} and $A_{aligned}$ (clones of 4–16 cells) spermatogonia (Buaas *et al*., 2004; Greenbaum *et al*., 2006; Tokuda *et al*., 2007; Schlesser *et al*., 2008). Neurogenin 3 (NGN3) is also expressed by both undifferentiated (A_{single}, A_{paired}, $A_{aligned}$) and differentiating spermatogonia (types A1–A4, intermediate and B) (Yoshida *et al*., 2004, 2007b), although NGN3 expression in $A_{singles}$ and transplantable stem cells is heterogeneous (Nakagawa *et al*., 2007; Yoshida *et al*., 2007a). In contrast, the cKIT receptor tyrosine kinase is absent from A_{single}, A_{paired} and most $A_{aligned}$ spermatogonia, but initiates expression in larger $A_{aligned}$ clones (8 and 16 cells) and continues in differentiating spermatogonia (types A1–A4, intermediate and B) (Manova *et al*., 1990; Sorrentino *et al*., 1991; Yoshinaga *et al*., 1991; Tajima *et al*., 1994; Dym *et al*., 1995; Schrans-Stassen *et al*., 1999). Thus, on the basis of whole-mount analyses, it is possible to assign molecular phenotypes to stem (A_{single} and some A_{paired}; GFRα1$^+$, PLZF$^+$, NGN3$^{+/-}$ and cKIT$^-$), progenitor (some A_{paired} and $A_{aligned}$; GFRα1$^+$, PLZF$^+$, NGN3$^+$, cKIT$^{+/-}$) and differentiating (A1–A4, intermediate, B; GFRα1$^-$, PLZF$^-$, NGN3$^+$ and cKIT$^+$) spermatogonia in rodents.

Rodent SSCs can also be identified retrospectively by their ability to initiate and maintain spermatogenesis in a functional transplantation assay that was originally described by Brinster and colleagues (Brinster and Avarbock, 1994; Brinster and Zimmermann, 1994). Fluorescence-activated cell sorting (FACS) combined with SSC transplantation has enabled systematic characterization of mouse SSCs as a subpopulation of mouse testis cells defined by the phenotype α6-Integrin (CD49f)$^+$, β1-Integrin (CD29)$^+$, THY-1 (CD90)$^+$, CD9$^+$, Hoechst side population$^+$, Rho123^{low}, αv-Integrin (CD51)$^-$, c-KIT (CD117)$^-$, major histocompatibility complex class I (MHC-I)$^-$, and CD45$^-$ (Shinohara *et al*., 1999, 2000; Kubota *et al*., 2003; Falciatori *et al*., 2004; Kanatsu-Shinohara *et al*., 2004; Lassalle *et al*., 2004; Fujita *et al*., 2005; Lo *et al*., 2005).

In contrast to rodents, very little is known about the molecular characteristics of non-human primate SSCs. Classical studies of nuclear morphology have described two types of undifferentiated (type A) spermatogonia in the non-human primate testis, designated A_{dark} and A_{pale} (Clermont and Leblond, 1959; Clermont, 1972; Cavicchia and Dym, 1978). Both cell types are present on the basement membrane of primate seminiferous tubules, but differ on the basis of nuclear architecture and staining intensity with hematoxylin. There is limited information about the clonal arrangement of A_{dark} and A_{pale} spermatogonia (Clermont and Leblond, 1959; Ehmcke *et al*., 2005) or how these histological phenotypes correlate with the molecular characteristics of rodent spermatogonia. The prevailing model of spermatogonial proliferation and differentiation in primates is that A_{dark} and A_{pale} represent reserve and renewing stem cells, respectively (Clermont, 1969; Clermont and Antar, 1973; Fouquet and Dadoune, 1986; van Alphen and de Rooij, 1986; Plant and Marshall, 2001; Ehmcke *et al*., 2005; Simorangkir *et al*., 2005). According to this 'reserve stem cell' model, A_{pale} are the renewing stem cells that undergo regular divisions to maintain a pool of undifferentiated germ cells and support spermatogenesis under normal circumstances. A_{dark} are reserve stem cells that, in the adult, rarely divide and are activated when spermatogenesis is destroyed by radiation (van Alphen and de Rooij, 1986). However, these reserve and renewing stem cell designations require confirmation through additional experimentation.

In the current study, we utilized rhesus-to-nude mouse xenotransplantation as a biological assay to investigate SSCs in FACS-sorted rhesus testis cell suspensions (Hermann *et al*., 2007). To further dissect the molecular signature of rhesus spermatogonia, we performed immunohistochemistry for consensus rodent SSC markers in juvenile and adult rhesus testes. Initial studies focused on juvenile macaques because the only germ cells present at this stage of testis development are A_{dark} and A_{pale} spermatogonia (Ramaswamy *et al*., 2000b; Simorangkir *et al*., 2005), simplifying gating in FACS experiments and identification of type-A spermatogonia in tissue sections. Adult macaques were employed in subsequent studies to gain insights about SSCs and the spermatogenic lineage in the context of the fully developed adult tissue. Collectively, these experiments allowed us to phenotypically identify putative SSCs in rhesus testes.

Materials and Methods

Experimental animals

Twelve juvenile (14–28 months of age) and eight adult rhesus macaques from both Indian and Chinese ancestry were used for these studies. Macaques were housed under a constant light-dark cycle (12–12 h). All experiments utilizing animals were approved by the Institutional Animal Care and Use Committee of the University of Pittsburgh (which is also the IACUC of record for Magee-Womens Research Institute, assurance no. A3654-01) and were performed in accordance with the NIH Guide for the Care and Use of Laboratory Animals.

Preparation of donor juvenile rhesus macaque testis cell suspensions

Donor cells were recovered from juvenile rhesus testis tissue collected by castration or hemicastration using a modified two-step enzymatic digestion procedure, as described previously for adult rhesus testis cells (Hermann *et al*., 2007). This cell isolation procedure yielded an average of $503 \pm 48 \times 10^6$ testis cells per gram of juvenile rhesus testis parenchyma with a viability of $97 \pm 0.3\%$. In some experiments, testis cells were analyzed

and sorted by FACS, stored overnight at 4°C in medium gassed with 5% CO_2 and xenotransplanted the following day (fresh cells). In other experiments, cells were cryopreserved immediately after isolation and thawed later, as described (Hermann *et al*., 2007). Cryopreserved cells were used for FACS analysis and xenotransplantation as described for fresh cells. Cryopreserved testis cells from all 12 juveniles were thawed after an average storage duration of 151 ± 27 days in liquid nitrogen and were recovered at an average efficiency of 76.6 ± 3.8% and a viability of 80.8 ± 0.9%.

THY-1 FACS

Juvenile rhesus testis cells were suspended ($5–20 \times 10^6$ cells/ml) and stained with the THY-1 primary antibody (0.5 μg/10^6 cells; APC conjugate; BD Biosciences, San Jose, CA, USA) on ice in Dulbecco's phosphate-buffered saline (DPBS) containing 10% FBS (DPBS + S). Staining was compared with an isotype control antibody (mouse IgG1κ-APC, BD Biosciences) to correct for non-specific binding. Propidium iodide (0.5 μg/ml, BD Biosciences) was added for discrimination of dead cells. Evaluation of antibody staining by flow cytometry and cell sorting by FACS was performed using a FACSvantage SE (BD, Franklin Lakes, NJ, USA).

VASA immunocytochemistry

For immunocytochemical detection of VASA (DDX4) in suspensions of juvenile rhesus testis cells (unsorted and sorted THY-1^+ and THY-1^- fractions), approximately 1×10^4 cells from each cell suspension were spotted onto glass slides. Cells were fixed (7:1 v/v ethanol:glacial acetic acid) and dried. Spotted cells were rehydrated with DPBS, blocked in antibody diluent (DPBS + 0.1% Triton X-100, 5% normal serum from host species of secondary antibody, 3% BSA) and incubated with the VASA primary antibody in antibody diluent [rabbit anti-VASA IgG (DDX4, 1:200 dilution; ab13840, Abcam, Cambridge, MA, USA)]. The primary antibody was detected with goat anti-rabbit IgG AlexaFluor488 (1:200; Invitrogen, Carlsbad, CA, USA). Samples were mounted with VectaShield mounting media containing DAPI (Vector Laboratories, Burlingame, CA, USA) and visualized on an E600 fluorescent microscope (Nikon USA, Melville, NY, USA) equipped with an X-Cite 120 fluorescence excitation source (EXFO Life Sciences, Ontario, Canada). Digital images were acquired using a Spot RT Slider cooled CCD digital camera (Diagnostic Instruments, Sterling Heights, MI, USA) and MetaVue software (Molecular Devices, Sunnyvale, CA, USA). The number of VASA$^+$ cells was counted in 10 random microscopic fields for each cell population and the percentage expressing VASA was calculated by dividing the number of labeled cells by the total number of DAPI$^+$ cells in the same fields (average 928 ± 114 total cells counted per population per experiment). Statistically significant differences in VASA staining between the unsorted, THY-1^+ and THY-1^- cell populations were determined by Student's *t*-test.

Quantitative RT–PCR for SSC marker mRNA assessment

Total RNA was isolated from unsorted and THY-1 FACS-sorted testis cells from three juvenile rhesus macaques with Trizol reagent (Invitrogen) according to manufacturer recommendations, and 0.5 μg was used for cDNA synthesis in the presence and absence of Super Script III reverse transcriptase (Invitrogen) and oligo-dT_{18} primer. The resulting cDNAs were used in quantitative PCR reactions. Primers for cDNA amplification were designed with Primer Express software (v3.0, Applied Biosystems, Foster City, CA, USA) and validated for 90–100% efficiency. Primers for cDNA amplification by quantitative RT–PCR were as follows: *GAPDH* (accession no. XM_001105471, 5′-CCATCTTCCAGGAGCGAGATC-3′ and 5′-GCTCCCCCCTGCAAATG-3′), *PLZF* (accession no. XM_001086244; 5′-AGCGGTTCCTGGATAGTTTGC-3′ and 5′-TTCGAAAACTGTGCACCACACT-3′), *GFRα1* (accession no. XM_001094722; 5′-GGGAGAAGCCCAACTGTTTG-3′ and 5′-GACAGCTGCTGACAGACCTTGA-3′), *VASA* (accession no. XM_001100045; 5′-GAAGCTGATCGCATGTTGGATA-3′ and 5′-TGCAGCCAACCTTTGAATTTC-3′). Quantitative PCR reactions were carried out in triplicate for each sample and primer set using *Power* SYBR green PCR master mix (Applied Biosystems), 12.5 ng cDNA per reaction and 250 nM primer concentration on a 7900HT Fast Real-Time PCR System (Applied Biosystems). *GAPDH* cDNA amplification was used for normalization. An amplification efficiency standard curve was run in each assay. The relative abundance of each target gene was calculated using the ΔΔCt method, where the mean Ct of the gene of interest (i.e. *PLZF*, *GFRα1* or *VASA*) for each sample was divided by the mean Ct of *GAPDH* for that sample. Each of the resulting ΔCt values for a given animal, cell population and gene was divided by the ΔCt of the unsorted control sample for that animal, cell population, and gene, producing a ΔΔCt, which was used to determine the fold-change value ($2^{-\Delta\Delta Ct}$).

Rhesus-to-nude mouse xenotransplantation assay for SSCs

Rhesus-to-nude mouse xenotransplantation was used as a biological assay to investigate rhesus SSCs and was performed as described previously (Hermann *et al*., 2007). Briefly, recipient nude mice (NCr nu/nu; Taconic, Germantown, NY, USA) were treated with busulfan (40 mg/kg; Sigma) at 5–6 weeks of age (5–8 weeks prior to donor cell transplantation) to eliminate endogenous spermatogenesis (Bucci and Meistrich, 1987; Brinster and Avarbock, 1994). Approximately 7 μl of donor testis cell suspension (unsorted or sorted fractions) containing 10% trypan blue (Invitrogen) at $1–120 \times 10^6$ cells/ml (depending on cell population and experiment) was injected into the seminiferous tubules of recipient testes via the efferent ducts (Ogawa *et al*., 1997). For quantitative analysis of donor spermatogonia colonization, intact seminiferous tubules were prepared from nude mouse recipient testes, collected 2 months after transplantation, fixed, and all recovered tubules were stained in whole-mount with the rhesus testis cell antibody as described (Hermann *et al*., 2007). The rhesus testis cell antibody, which was detected by indirect fluorescent immunohistochemistry (see what follows), specifically recognizes engrafted primate cells in recipient mouse seminiferous tubules, as demonstrated in our previous report by western blot and staining seminiferous tubules from sham transplanted control mice (Hermann *et al*., 2007). Seminiferous tubules from each recipient mouse testis were also systematically evaluated for rhesus donor-derived spermatogonial colonies. Putative stem cell-derived donor colonies of rhesus spermatogonia meeting the following criteria were counted: at least four cells exhibiting spermatogonial morphology (ovoid shape with high nuclear to cytoplasmic ratios) located on the basement membrane in a continuous area of recipient seminiferous tubule (≤100 μm between cells). Colonization foci that did not meet all of these criteria were not counted. In many cases, cells within donor-derived colonies were arranged in chains connected by intercellular cytoplasmic bridges. The colonization data exhibited non-normal distribution, and the measurements within each replicate were dependent. Therefore, to compare between groups (unsorted, THY-1^+ and THY-1^-), we calculated a *t*-statistic for each replicate [$T_i = (X_i - Y_i)/N_i$], where *T* is the percentage of measurements where one group is higher than the other (X_i/N_i), minus the percentage where the latter group is higher than the first (Y_i/N_i). Then a non-parametric one-sample, one-sided Wilcoxon signed-rank test was applied to the *t*-statistics to identify significant differences in colonization activity between groups. One-sided analysis was justified because THY-1 is an established marker of SSCs (Kubota *et al*., 2003; Ryu *et al*., 2004).

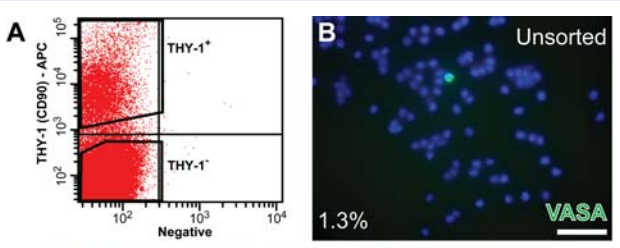

E

Fraction	% Gated	Viability (%)	Sort Purity (% in gate)	VASA+ (%)
Unsorted	N/A	77.6 ± 3.4	N/A	1.3 ± 0.4
THY-1+	14.8 ± 3.5	82.8 ± 3.1	92.2 ± 1.6	9.2 ± 2.3
THY-1-	82.2 ± 3.4	86.2 ± 2.8	98.7 ± 0.3	0.08 ± 0.05

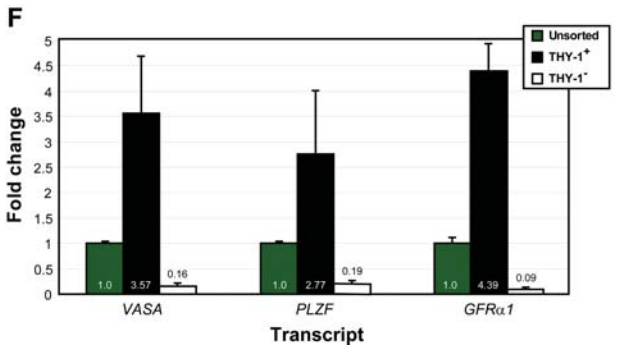

Figure 1 Rhesus testis cells expressing germ cell and SSC markers are enriched in the THY-1$^+$ fraction. (**A**) Juvenile rhesus testis cells were stained with a THY-1 (CD90) antibody and sorted using FACS into two fractions, THY-1$^+$ and THY-1$^-$ (polygons). Immunofluorescent staining for VASA (green) was performed in (**B**) unsorted, (**C**) FACS-sorted THY-1$^+$ and (**D**) FACS-sorted THY-1$^-$ testis cells spotted on glass slides. Cells were counterstained with DAPI (blue). The mean percentage of VASA$^+$ cells in each fraction from all replicates is shown in the bottom left of each image. Images are from stained fresh cells. Scale bars: 50 μm. (**E**) Mean (±SEM) cell sorting statistics from 12 independent FACS experiments (8 animals, using both fresh and cryopreserved cells) are shown for each population. Sort purity is defined as the percentage of sorted cells that fall into the respective sort gate upon re-analysis. The mean (±SEM) percentage of VASA$^+$ cells in unsorted and sorted cells is indicated in the last column. (**F**) Quantitative RT–PCR measured levels of *VASA*, *PLZF* and *GFRα1* mRNA from unsorted (green bars), THY1$^+$ (black bars) and THY-1$^-$ (white bars) testis cells. Data are presented as the mean (±SEM) fold-change for each gene relative to the mean levels in the unsorted population (three replicate experiments). Fold-change values were determined by the ΔΔCt method, where levels of each gene were normalized to *GAPDH*.

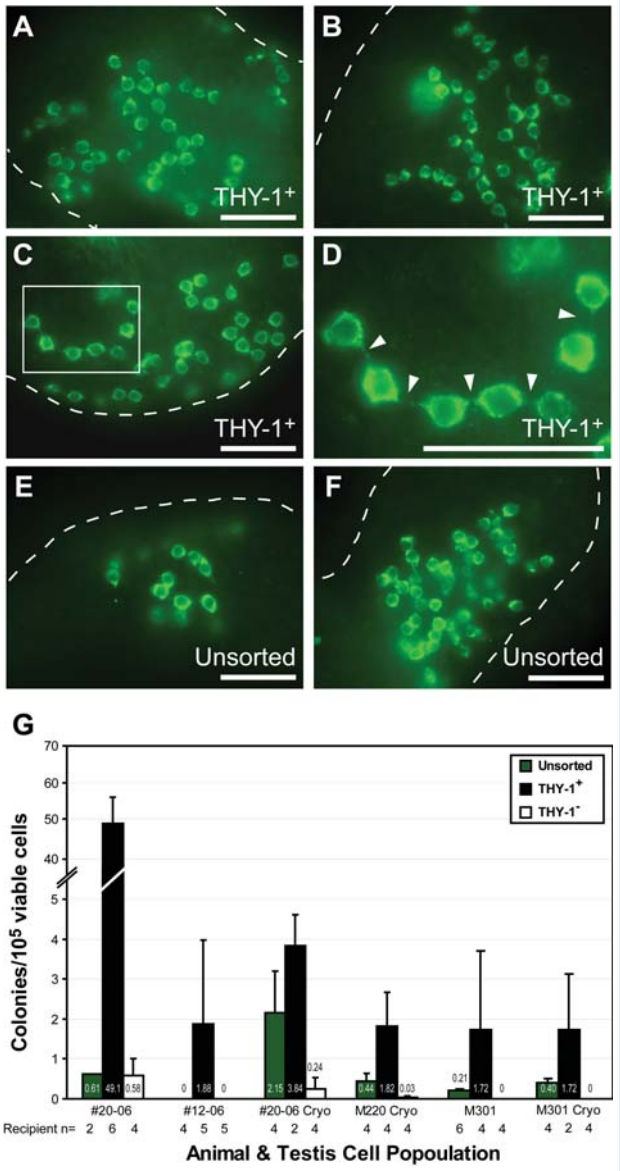

Figure 2 THY-1$^+$ rhesus testis cells have enhanced xenotransplant colonizing activity. (**A**–**F**) The rhesus-to-nude mouse xenotransplantation assay was used to investigate SSCs by detecting donor-derived spermatogonial colonies that arise from transplanted rhesus testis cells (Hermann *et al*., 2007). White box in (C) is enlarged in (D), and white arrowheads mark characteristic intercellular cytoplasmic bridges in chains of rhesus spermatogonia. Representative colonies from (A–D) THY-1$^+$ and (E and F) unsorted donor cells are shown and the source of donor cells is noted. Dashed white lines mark seminiferous tubule margins. Scale bars: 50 μm. (**G**) Colonization results from the xenotransplant assay are shown for unsorted (green bars) and FACS-sorted [THY-1$^+$ (black bars) and THY-1$^-$ (white bars)] juvenile rhesus testis cells from four animals in six sorting experiments. Results from each experiment are presented as the mean (±SEM) number of xenotransplant colonies per 10^5 viable cells transplanted. The number of recipient mouse testes analyzed is shown below each bar.

Immunohistochemistry and nuclear morphology analyses in rhesus testes

Testicular fragments from juvenile and adult rhesus macaques were fixed with 4% paraformaldehyde, paraffin-embedded and sectioned (5 μm). For immunohistochemistry, tissue sections were deparaffinized, rehydrated, subjected to antigen retrieval in sodium citrate buffer (10 mM sodium citrate, pH 6.0, 0.05% Tween-20) or EDTA buffer (1 mM EDTA, pH 8.0, 0.05% Tween-20), rinsed and blocked in antibody diluent. Subsequently, sections were stained with the following primary antibodies in antibody diluent: anti-VASA, anti-PLZF (ZBTB16, 1:800; Hobbs and Pandolfi; Hermann *et al.*, 2007), anti-human cKIT (1:800; A4502, DakoCytomation, Carpinteria, CA, USA; Gaskell *et al.*, 2004), anti-NGN3 (1:5000; ab54743, Abcam) or anti-GFRα1 (1:250; MAB7141, R&D Systems, Minneapolis, MN, USA). Staining specificity for each individual antibody was validated by comparison with two negative controls: (i) normal non-immune (isotype control) IgGs (all from BD Biosciences) and (ii) omission of primary antibody (Supplementary Material, Fig. S1). For immunohistochemistry experiments reported in Figs 3–6, positive immunoreactivity was validated by omission of primary antibody.

For fluorescent co-staining experiments, primary antibodies were detected with the following secondary antibodies: biotinylated goat anti-Armenian hamster IgG (Jackson Immunoresearch Laboratories, West Grove, PA, USA) plus AlexaFluor 488-conjugated streptavidin (Invitrogen) goat anti-Armenian Hamster IgG Rhodamine RedX (Jackson Immunoresearch Laboratories) and goat anti-rabbit AlexaFluor488 IgG, goat anti-rabbit AlexaFluor568 IgG, goat anti-mouse AlexaFluor488 IgG and goat anti-mouse AlexaFluor568 IgG (all from Invitrogen). Fluorescently stained sections were mounted with VectaShield mounting media containing DAPI (Vector Laboratories) and imaged. For the quantification of marker overlap, single-positive cells for each marker and double-positive cells were counted in cross-sections of seminiferous cords (juvenile) or seminiferous tubules (adult). Total stained cell numbers were divided by the number of cross-sections (at least 100 per animal). For colorimetric detection of VASA, NGN3, GFRα1 and cKIT, primary antibodies were as mentioned earlier for immunofluorescence and were detected with EnVision+ System HRP DAB staining kits for mouse and rabbit primary antibodies (DakoCytomation) according to manufacturer recommendations. For colorimetric detection of PLZF, the primary antibody was detected with biotinylated goat anti-Armenian hamster secondary antibody (Jackson Immunoresearch Laboratories) and colorimetric detection using the DAB Histochemistry kit with streptavidin HRP (Invitrogen) according to manufacturer recommendations. Sections were then counterstained using the periodic acid-Schiff method (Sigma-Aldrich) and Gills hematoxylin (Sigma-Aldrich), as described (Simorangkir *et al.*, 2003), to identify undifferentiated and differentiating spermatogonia on the basis of nuclear morphology (i.e. A_{dark}, A_{pale}, B1-B4 spermatogonia) and seminiferous tubule stage. Counterstained sections were dehydrated, cleared and mounted with CytoSeal XYL (Richard Allen Scientific, Kalamazoo, MI, USA). The number of labeled and unlabeled A_{dark} and A_{pale} spermatogonia in stained sections was then determined for each testis sample, and the labeling index of each cell type was calculated by dividing the number of labeled cells by the sum of both labeled and unlabeled cells and then expressed as a percentage for each sample.

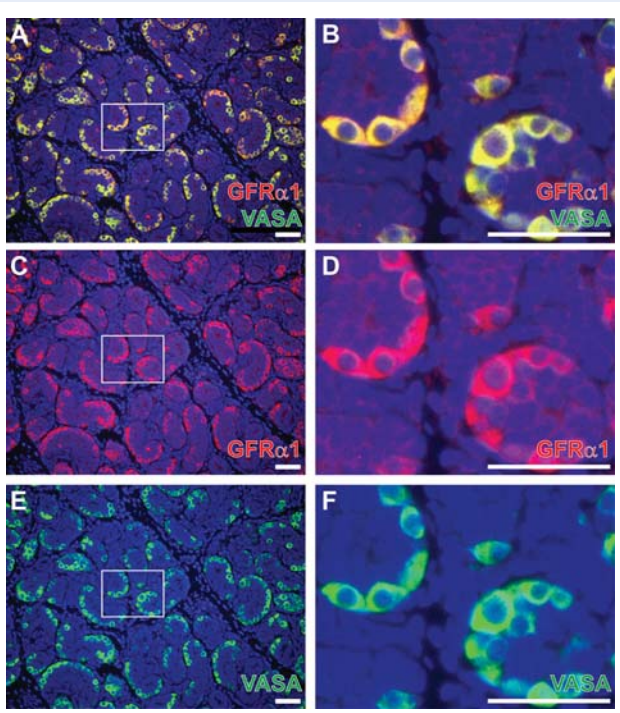

Figure 3 All VASA$^+$ germ cells are GFRα1$^+$ in the juvenile rhesus testis. To characterize the expression of GFRα1 in juvenile rhesus testes, we performed immunohistochemical co-staining for (**A** and **B**) GFRα1 and the pan germ cell marker VASA in sections of juvenile rhesus testes. Individual staining profiles are also shown for (**C** and **D**) GFRα1 and (**E** and **F**) VASA. In all images, DAPI counterstain (blue) identifies all cell nuclei. The white box in the first image (e.g. A) is enlarged in the second image (e.g. B). Markers are noted on each image in the color of the corresponding fluorophore. Scale bars: 50 μm.

Results

Rhesus spermatogonia expressing the stem cell marker, THY-1, have enhanced colonizing activity

THY-1 is a marker of mouse and rat SSCs (Kubota *et al.*, 2003; Ryu *et al.*, 2004), as well as mouse, rat and human hematopoietic stem cells (Goldschneider *et al.*, 1978; Spangrude *et al.*, 1988; Baum *et al.*, 1992). Therefore, we hypothesized that THY-1 is also a marker of rhesus SSCs and evaluated the expression of this cell-surface marker by FACS. Juvenile testis cell suspensions stained with a THY-1 antibody contained two discrete cell populations, designated THY-1$^+$ and THY-1$^-$ (Fig. 1A). The THY-1$^+$ and THY-1$^-$ fractions represented 14.8 ± 3.5 and 82.2 ± 3.4%, respectively, of juvenile testis cells (n = 12 experimental sorts using cells from 8 juveniles) and were similar in fresh cells (13.3 ± 7% THY-1$^+$ and 83.7 ± 7% THY-1$^-$; 5 fresh cell sorts from 5 juveniles) and cryopreserved cells (16 ± 4.3% THY-1$^+$ and 81.1 ± 4.1% THY-1$^-$; 7 cryopreserved cell sorts from 6 juveniles; $P = 0.73$). Immunofluorescent staining revealed that 1.3% of unsorted juvenile rhesus testis cells express the pan germ cell marker, VASA (Fig. 1B and E). VASA$^+$ cells were significantly enriched in the THY-1$^+$ fraction (9.2%, $P = 0.0045$, Fig. 1C and E) with corresponding depletion in the THY-1$^-$ fraction (0.08%, $P = 0.0056$, Fig. 1D and E). To further characterize the THY-1$^+$ fraction, quantitative RT–PCR was used to evaluate mRNA levels of *VASA* as well as *GFRα1* and *PLZF*, two consensus markers of mouse stem and progenitor

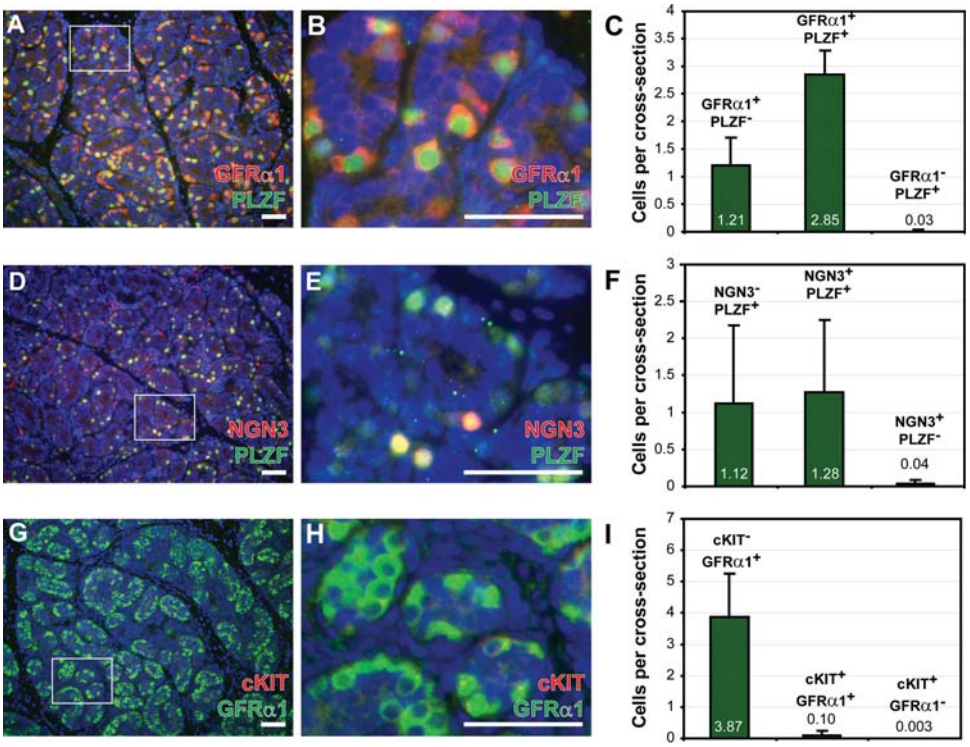

Figure 4 GFRα1, PLZF and NGN3 are expressed in spermatogonia of juvenile rhesus testes; cKIT is not expressed. We performed immunohistochemical co-staining for (**A**–**C**) GFRα1 and PLZF, (**D**–**F**) NGN3 and PLZF and (**G**–**I**) cKIT and GFRα1 in sections of juvenile rhesus testes. DAPI counterstain (blue) identifies all cell nuclei. For each marker combination, the area marked by a white box in the first image (e.g. A) is enlarged in the second image (e.g. B). Markers are noted on each image in the color of the corresponding fluorophore. Scale bars: 50 μm. The quantity and relative proportion of cells expressing each pair of markers are indicated in graphs in (C) GFRα1 and PLZF, (F) NGN3 and PLZF or (I) cKIT and GFRα1. Quantification is presented as the mean (±SEM) number of cells per seminiferous cord cross-section exhibiting the staining phenotype noted above the bars. A minimum of 100 seminiferous cord cross-sections per animal were analyzed from three juvenile rhesus macaques.

spermatogonia. Like *VASA*, the expression of both *PLZF* and *GFRα1* was enriched in the THY-1$^+$ fraction and reduced in the THY-1$^-$ fraction, relative to the unsorted testis cell suspension (Fig. 1F).

To evaluate functional correlates of THY-1 expression in rhesus spermatogonia, colonizing activity in THY-1 sorted and unsorted testis cell suspensions was assessed using the rhesus-to-nude mouse xenotransplantation assay. Colonies are considered to arise from SSCs because donor cells migrate to the basement membrane of recipient mouse seminiferous tubules, proliferate to produce colonies of spermatogonia connected by intercellular cytoplasmic bridges and persist for at least 2 months [the time of analysis (Hermann *et al.*, 2007); see Fig. 2A–F]. Representative colonies from THY-1$^+$ cells (Fig. 2A–D) and unsorted cells (Fig. 2E and F) are shown. Colonizing activity was significantly increased in the THY-1$^+$ fraction ($P = 0.0445$) and decreased or absent in the THY-1$^-$ fraction ($P = 0.0239$) relative to unsorted controls. Colonizing activity followed the same trend in six replicate xenotransplant experiments from four donor juveniles (Fig. 2G). The trend in relative colonizing activity between unsorted, THY-1$^+$ and THY-1$^-$ cell suspensions was similar in both fresh and cryopreserved testis cells (Fig. 2G), although the absolute number of colonies from fresh and cryopreserved cells of a given donor was not always the same (compare fresh versus frozen results of donor 20–06 and M301, Fig. 2G).

Rhesus type-A spermatogonia express consensus markers of rodent stem and progenitor spermatogonia

To further explore the molecular signature of rhesus spermatogonia, we evaluated the expression of VASA (pan germ cell marker), as well as GFRα1, PLZF and NGN3, consensus markers of stem and progenitor spermatogonia in rodents (Meng *et al.*, 2000; Buaas *et al.*, 2004; Costoya *et al.*, 2004; Buageaw *et al.*, 2005; Ryu *et al.*, 2005; Nakagawa *et al.*, 2007) in sections of paraformaldehyde-fixed juvenile testes. All four markers (VASA, GFRα1, PLZF and NGN3) were expressed in undifferentiated spermatogonia of juvenile rhesus testes (Figs 3 and 4). Co-staining for VASA and GFRα1 indicated that GFRα1 was present in all juvenile rhesus spermatogonia (i.e. all A_{dark} and A_{pale}; Fig. 3). Overlap of PLZF with GFRα1, however, was incomplete. PLZF was present in 70% of GFRα1$^+$ spermatogonia (Fig. 4A–C). We observed very few PLZF$^+$ spermatogonia that did not express GFRα1 (Fig. 4C). NGN3 exhibited the most restricted expression in the juvenile rhesus testis and was observed in only 53% of PLZF$^+$ germ cells (Fig. 4D–F). Again, we observed very few NGN3$^+$ cells that did not also express PLZF (Fig. 4F). cKIT is a marker of differentiating spermatogonia in rodents and, as expected, was essentially absent in juvenile rhesus testes, which contain only undifferentiated A_{dark} and A_{pale} (Fig. 4G–I).

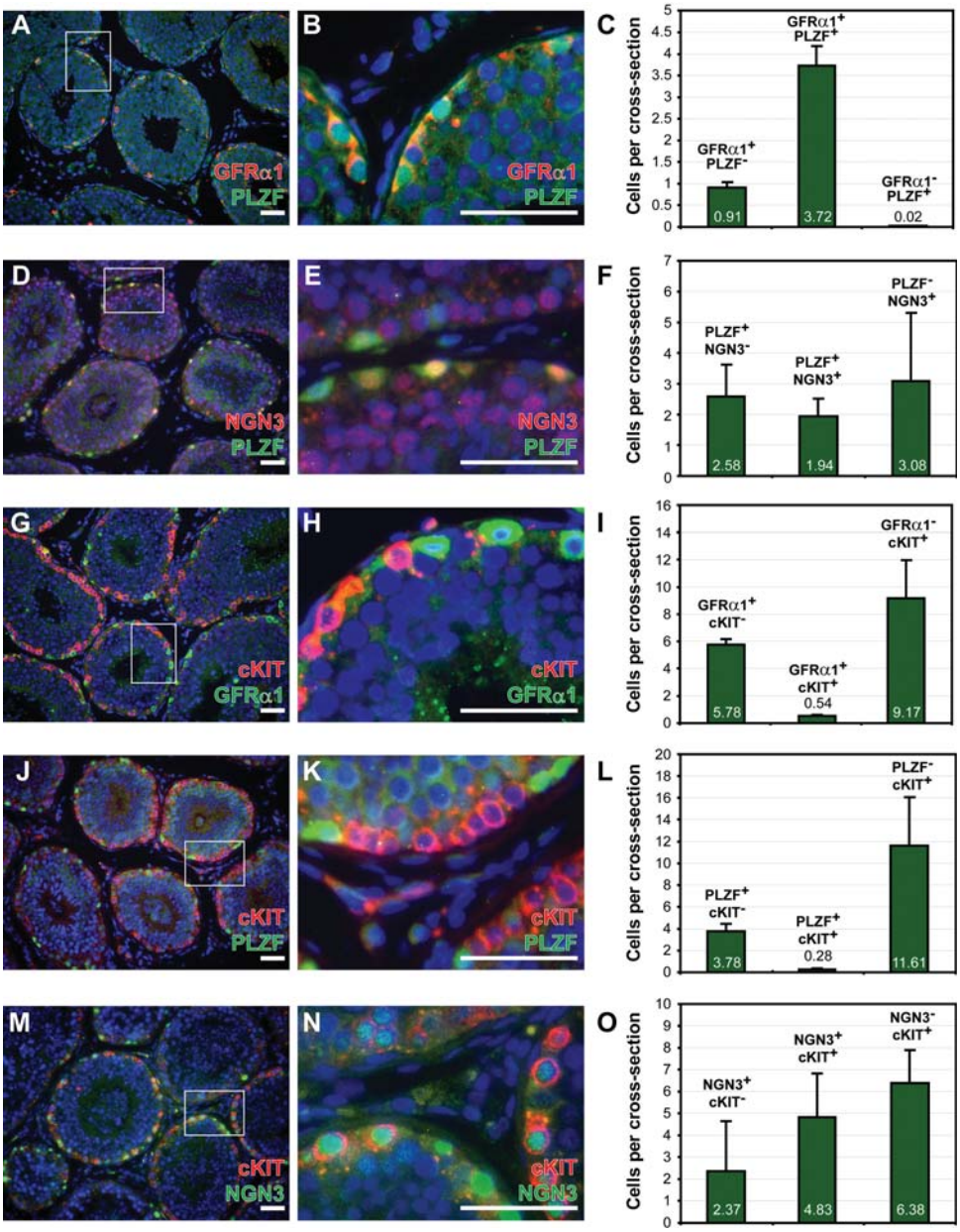

Figure 5 Differential overlap in the expression between putative markers of stem and/or progenitor spermatogonia (GFRα1, PLZF, NGN3) and cKIT in the adult rhesus testis. We performed immunohistochemical co-staining for (**A**–**C**) GFRα1 and PLZF, (**D**–**F**) NGN3 and PLZF, (**G**–**I**) cKIT and GFRα1, (**J**–**L**) cKIT and PLZF, (**M**–**O**) cKIT and NGN3 in sections of adult rhesus testes. The quantity and relative proportion of cells expressing each pair of markers from three adults are indicated for (C) GFRα1 and PLZF, (D) NGN3 and PLZF, (I) cKIT and GFRα1, (L) cKIT and PLZF, (O) cKIT and NGN3. Quantification of markers per seminiferous tubule cross-section and figure organization is as shown for Fig. 4.

Molecular dissection of the rhesus spermatogenic lineage in adults

The incomplete overlap of expression among GFRα1, PLZF and NGN3 in juvenile rhesus testes suggested that there may be subpopulations of type-A spermatogonia with distinct molecular phenotypes. To explore the expression of these spermatogonial markers during spermatogenesis, similar co-staining experiments were conducted on sections from adult rhesus testes. The relative expression relationships among GFRα1, PLZF and NGN3 observed in the juvenile were largely maintained in the adult testis (Fig. 5). GFRα1 and PLZF were restricted to cells on the seminiferous tubule basement membrane, as observed previously (Hermann *et al.*, 2007), and exhibited a high degree of overlap (80%; Fig. 5A–C). Overlap between PLZF and NGN3 ($PLZF^+NGN3^+$/total $PLZF^+$) was lower in adult testes than in juvenile testes (26% adult versus 52% juvenile). Also, a substantial proportion of adult $NGN3^+$ cells did not express PLZF (61%; Fig. 5D–F), unlike the juvenile, where such

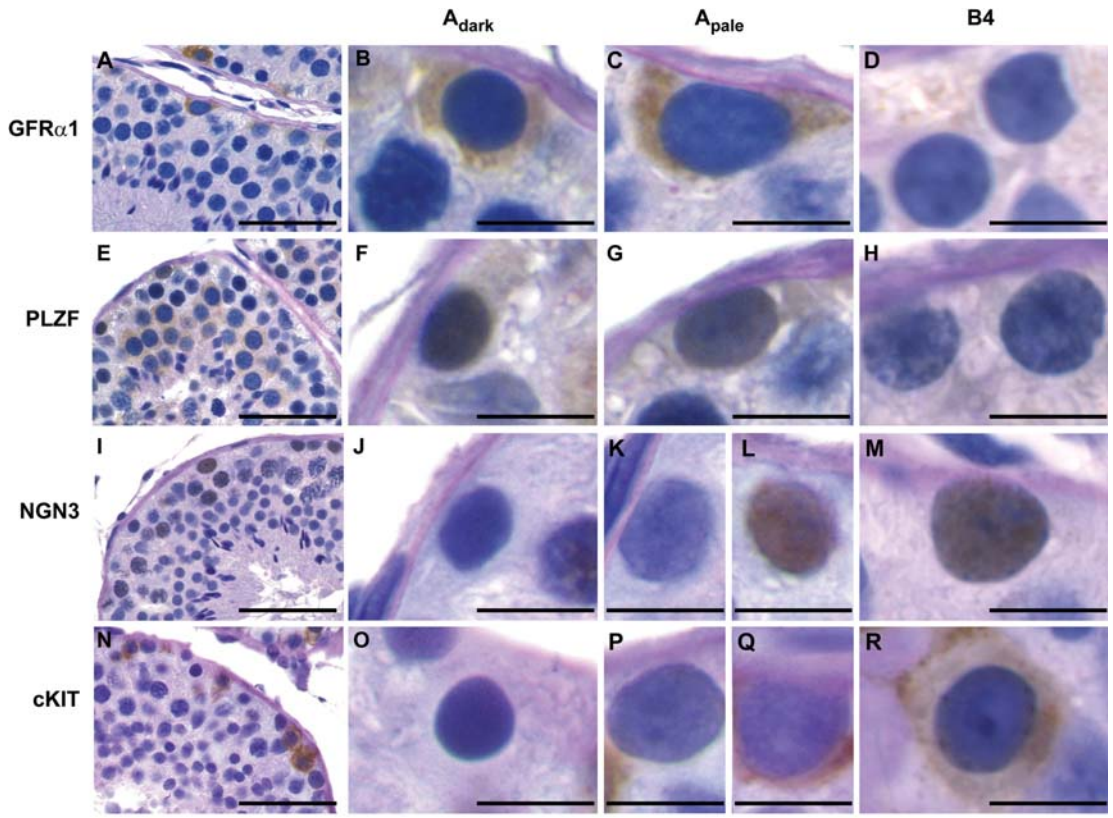

S

Label	A_{dark} (%)	A_{pale} (%)
GFRα1	100	100
PLZF	81.5±6.0	100
NGN3	0	48.5±2.7
cKIT	0	22.8±2.0

Figure 6 Correlation between molecular markers (GFRα1, PLZF, NGN3, cKIT) and morphological descriptions of spermatogonia (A_{dark}, A_{pale}, B) in the adult rhesus testis. Sections of adult rhesus testes were evaluated by immunohistochemistry for (**A**–**D**) GFRα1, (**E**–**H**) PLZF, (**I**–**M**) NGN3 and (**N**–**R**) cKIT. Subsequently, sections were counterstained by the PAS-hematoxylin method to reveal nuclear morphology and identify A_{dark} and A_{pale} spermatogonia, as well as differentiating type-B spermatogonia. The first image in each row (A, E, I, N) shows part of one seminiferous tubule cross-section (scale bar: 50 μm). Enlargements are also shown of representative A_{dark} (B, F, J, O), A_{pale} (C, G, K, L, P, Q) and B4 spermatogonia (D, H, M, R) (scale bar: 10 μm). (**S**) For all spermatogonia classified as A_{dark} or A_{pale}, the mean labeled percentage (±SEM) for the indicated marker is shown. Quantification was performed on an average of 1088 cells per marker from four adult rhesus macaques.

cells were infrequent (3%; Fig. 4F). These observations may reflect a difference between an expanding germ cell compartment in the developing testes of juveniles (Simorangkir *et al*., 2005) and the dynamic equilibrium of established spermatogenesis in the adult. To gain further insights about the sequential expression of these spermatogonial markers, co-staining experiments with cKIT were conducted on sections from adult rhesus testes. GFRα1 and PLZF exhibited limited overlap (<10%) with cKIT (Fig. 5G–L). In contrast, NGN3 exhibited appreciable overlap with cKIT; 67% of $NGN3^+$ cells also expressed cKIT (Fig. 5M–O). However, overlap between NGN3 and cKIT was incomplete because we observed $NGN3^+/cKIT^-$ cells as well as $NGN3^-/cKIT^+$ cells (Fig. 5O). Therefore, NGN3 appears to mark the transition from undifferentiated ($cKIT^-$) to differentiating ($cKIT^+$) spermatogonia in the adult rhesus testis. This is in apparent contradiction with previous mRNA *in situ*-hybridization experiments in mice that demonstrated limited overlap between *Ngn3* and *cKit* (Yoshida *et al*., 2004). However, the same investigators reported that *Ngn3* is expressed in larger clones of $A_{aligned}$ spermatogonia in mice (8, 16 and 32 cells) as well as in differentiating types A1–A4, intermediate and B spermatogonia (Yoshida *et al*., 2004, 2007b) that are known to express cKIT (Manova *et al*., 1990; Sorrentino *et al*., 1991; Yoshinaga *et al*., 1991; Tajima *et al*., 1994; Dym *et al*., 1995; Schrans-Stassen *et al*., 1999).

Correlating molecular phenotypes with morphological descriptions of rhesus spermatogonia

In order to understand the molecular phenotypes of rhesus spermatogonia in the context of classical descriptions of nuclear morphology (i.e. A_{dark}, A_{pale}, B spermatogonia), expression patterns of GFRα1, PLZF, NGN3 and cKIT were evaluated using colorimetric immunohistochemistry in adult testis sections counterstained by the periodic acid-Schiff method and hematoxylin. This analysis demonstrated that GFRα1 marks all A_{dark} and A_{pale} (Fig. 6A–D and S), consistent with our observations in juvenile testes (Fig. 3). GFRα1 staining was also observed in some B1 and B2 spermatogonia (not B3 or B4), but this labeling was not quantified. Similarly, PLZF stained almost all A_{dark} (81.5 ± 6%) and all A_{pale}, with limited labeling in B1 and B2 spermatogonia (not B3 or B4; Fig. 6E–H and S). In contrast, NGN3 staining was not detected in A_{dark}, present in only half of the A_{pale} pool and visible in nuclei of all B1, B2, B3 and B4 spermatogonia (Fig. 6I–M and S) and primary spermatocytes. cKIT staining was also absent from A_{dark}, but was observed in 22.8 ± 2% of A_{pale}, in all B spermatogonia (Fig. 6N–S) and in primary spermatocytes.

Discussion

In rodents, SSCs are defined experimentally by (i) their functional capacity to establish and maintain spermatogenesis in a transplantation assay (Ogawa *et al*., 1997; Nagano and Brinster, 1998), (ii) the expression of some or all of a battery of specific molecular markers [e.g. PLZF, GFRα1, UTF1, CDH1, NGN3, α6-Integrin (CD49f), β1-Integrin (CD29), THY-1 (CD90), CD9; Shinohara *et al*., 1999, 2000; Meng *et al*., 2000; Kubota *et al*., 2003; Buaas *et al*., 2004; Costoya *et al*., 2004; Kanatsu-Shinohara *et al*., 2004; Yoshida *et al*., 2004; Nakagawa *et al*., 2007; Tokuda *et al*., 2007; van Bragt *et al*., 2008] and (iii) their clonal arrangement (A_{single} and at least some A_{paired}) on the basement membrane of seminiferous tubules (de Rooij and Russell, 2000). In contrast, almost nothing was previously known about SSCs in primate testes. A_{dark} and A_{pale} are morphological descriptions and there is limited information about how these descriptions correlate with molecular characteristics. To begin addressing this deficit, we used FACS analysis, a rhesus-to-nude mouse xenotransplantation technique and immunochemical approaches to begin dissecting the phenotype and function of undifferentiated spermatogonia in juvenile and adult rhesus testes.

The combination of FACS analysis with immunocytochemistry, quantitative RT–PCR and xenotransplantation provided strong evidence that the THY-1 cell surface marker is conserved on rhesus SSCs. Notably, the THY-1$^+$ and THY-1$^-$ fractions of juvenile rhesus testis cells were clearly resolved, which facilitated assignment of gates for sorting. In contrast, similar analyses in mouse and rat testes in previous studies revealed more heterogeneous THY-1 expression profiles, and thus, assignment of gates was comparatively arbitrary (Kubota *et al*., 2003; Ryu *et al*., 2004). Rhesus-to-nude mouse xenotransplantation was employed as a biological assay to investigate SSCs (Hermann *et al*., 2007) and demonstrated segregation of colonizing activity to the THY-1$^+$ fraction. Colonizing activity from juvenile testis cells in the current study was similar to previous observations with adult rhesus testis cells (0.46 colonies per 10^5 viable cells; Hermann *et al*., 2007). Muller *et al*. (2008) recently reported that the glycan markers SSEA-4 and TRA-1-81 are present on the cell surface of rare rhesus spermatogonia. Future studies utilizing FACS and rhesus-to-nude mouse xenotransplantation could determine whether these glycan markers are observed on colonizing SSCs and also their degree of overlap with THY-1.

Molecular phenotyping identifies the putative rhesus SSC pool

Knowledge of rodent SSCs may provide clues about the identity of rhesus SSCs. The succession of marker expression in rodents is indicated at the bottom of Fig. 7 and provides a frame of reference that may allow the assignment of functional descriptors (i.e. stem, progenitor and differentiating spermatogonia) to phenotypically distinct subpopulations of cells in the adult rhesus spermatogenic lineage. Data from juvenile macaques are not incorporated in this summary because the juvenile testis lacks differentiating germ cells and corresponding data in rodents are unavailable. In mice, A_{single} and A_{paired} spermatogonia represent 0.03 and 0.06%, respectively, of germ cells in the testis (Tegelenbosch and de Rooij, 1993). In addition to A_{single} spermatogonia, at least some A_{paired} spermatogonia must be stem cells because they will complete cytokinesis (self-renew) to produce two new A_{single} spermatogonia (shaded as transition in Fig. 7). The proportion of A_{paired} that exhibit stem cell function is probably context-dependent and can range from all (0.06% of germ cells) to none, but is likely between these extremes. Therefore, the theoretical size of the SSC pool in rodents is between 0.03 and 0.09% of germ cells (0.03% from A_{single} + 0.06% from A_{paired}). A_{single} and A_{paired} are partially characterized by the phenotype GFRα1$^+$, PLZF$^+$ and cKIT$^-$ (reviewed in Aponte *et al*., 2005). NGN3 is also expressed by A_{single}, A_{paired} and other undifferentiated spermatogonia (Yoshida *et al*., 2004, 2007a, b), although it was recently observed that NGN3 expression in $A_{singles}$ is heterogeneous (Nakagawa *et al*., 2007), and this mixed phenotype may also be exhibited by transplantable SSCs (16, 63). Thus, it is reasonable to propose that the stem cell pool in mice (A_{single} and at least some A_{paired}) is comprised of cells with two distinct phenotypes (i.e. GFRα1$^+$, PLZF$^+$, NGN3$^-$, cKIT$^-$; GFRα1$^+$, PLZF$^+$, NGN3$^+$ and cKIT$^-$).

In the monkey, these two phenotypes (GFRα1$^+$, PLZF$^+$, NGN3$^-$, cKIT$^-$ and GFRα1$^+$, PLZF$^+$, NGN3$^+$, cKIT$^-$) are exhibited by most A_{dark} and ~75% of A_{pale} spermatogonia (Fig. 7, top). Assuming that molecular characteristics correlate with function and these relationships are evolutionarily conserved, the pool of putative rhesus SSCs could comprise as many as 3.5% of total germ cells in the rhesus testis [A_{dark} and A_{pale} each comprise ~2% of germ cells in the rhesus testis (Marshall and Plant, 1996; Ramaswamy *et al*., 2000a; Plant *et al*., 2005)]. Therefore, it appears that the putative stem cell pool in the monkey makes up a much larger proportion of the adult germ cell lineage than the stem cell pool in mice (3.5% versus 0.03–0.09%, depending on what proportion of A_{paired} are stem cells).

Direct functional evidence for the apparent differences in the size of rodent and primate SSC pools cannot be obtained with the transplantation approaches that are currently available. In rodents, SSC transplantation is a powerful functional assay for stem cells in which transplanted donor SSCs produce colonies of complete spermatogenesis in recipient testes with an efficiency of 5–12% (Dobrinski *et al*.,

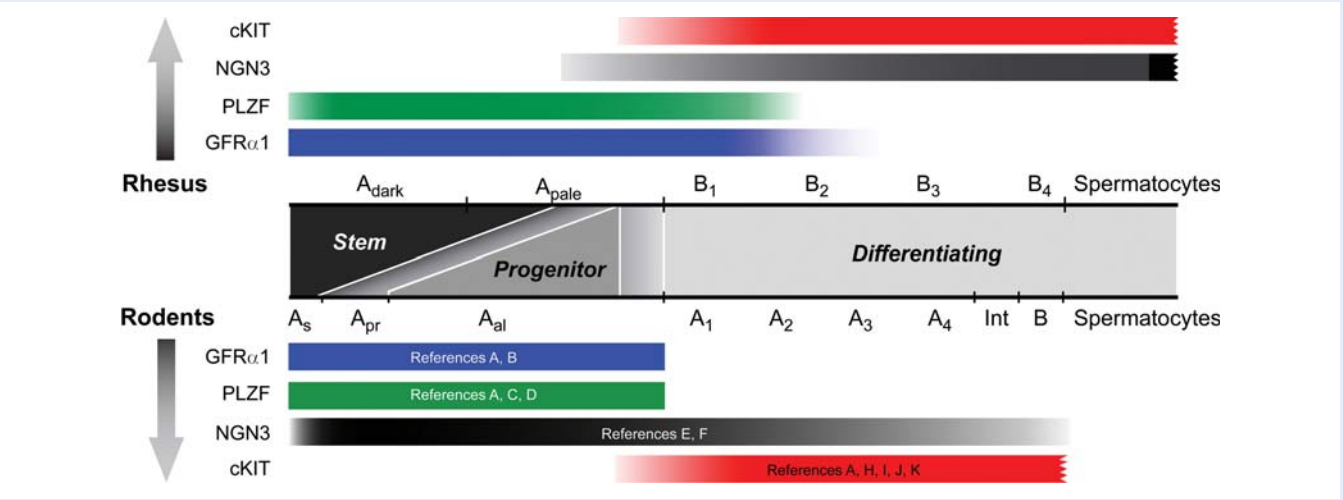

Figure 7 Summary of marker expression in the adult rhesus and mouse spermatogenic lineages. Colored bars (GFRα1, blue; PLZF, green; NGN3, black; cKIT, red) indicate the extent of marker expression in the adult spermatogenic lineage based on data from Figs 5 and 6 (rhesus, top) or review of the literature (rodents, bottom). Citations for rodent marker expression profiles are indicated within each bar and are as follows: A (Tokuda *et al*., 2007), B (Schlesser *et al*., 2008), C (Buaas *et al*., 2004), D (Greenbaum *et al*., 2006), E (Yoshida *et al*., 2004), F (Yoshida *et al*., 2007b), H (Manova *et al*., 1990), I (Sorrentino *et al*., 1991), J (Dym *et al*., 1995), K (Schrans-Stassen *et al*., 1999). 'Stem', 'Progenitor' and 'Differentiating' functional descriptors, based on rodent data, are indicated in the middle gray bar and may identify rhesus spermatogonia with corresponding phenotype and function. The transitions from stem to progenitor or progenitor to differentiating are noted by gradient shading between these functional categories. The following abbreviations are used for rodents: A_s, A_{single}; A_{pr}, A_{paired}; A_{al}, $A_{aligned}$.

1999; Nagano *et al*., 1999; Orwig *et al*., 2002; Nagano, 2003). Although rhesus-to-nude mouse xenotransplantation appears to be an assay of rhesus SSCs, the transplanted cells do not produce complete spermatogenesis and the efficiency of this assay is not known (Hermann *et al*., 2007). Complete spermatogenesis from donor rhesus SSCs may one day be demonstrated in a rhesus-to-rhesus transplantation paradigm, but homologous transplantation is unlikely to prove feasible as a quantitative biological assay because of high cost and biological variation among out-bred primates.

Relative to the respective stem cell pools, the progenitor pool appears much smaller in adult macaques than in rodents. We define progenitors as undifferentiated spermatogonia that are committed to differentiate and can undergo only a finite number of self-renewing divisions. In mice, the progenitor pool includes some A_{paired} and all $A_{aligned\ 4-16}$. These cells have the phenotype GFRα1$^+$, PLZF$^+$, NGN3$^+$ and cKIT$^{+/-}$ (Fig. 7, bottom) and comprise 89% of all undifferentiated spermatogonia (A_{single}, A_{paired}, $A_{aligned}$) in the mouse testis (Tegelenbosch and de Rooij, 1993). In contrast, this phenotype is observed in ~50% of monkey A_{pale} spermatogonia and thus comprises only 25% of the total undifferentiated spermatogonia (A_{dark} and A_{pale}) in the adult testis (Fig. 7, top). In this regard, it is noteworthy that adult rodent and adult rhesus testes both produce a similar number of sperm per gram of testis per day (Sharpe, 1994; Gupta *et al*., 2000; Thayer *et al*., 2001). Therefore it may be concluded that the stem/progenitor cell pools in primates and rodents employ different strategies to meet a similar biological demand. Rodents have a small stem cell pool and a relatively larger pool of transit-amplifying progenitors, whereas rhesus testes appear to have a larger stem cell pool with a relatively smaller transit-amplifying progenitor compartment. Additional studies are needed to determine whether the larger putative SSC pool in rhesus is a feature shared by other primate species, including humans.

Correlating molecular phenotypes with classical A_{dark} and A_{pale} descriptions of nuclear morphology in adult rhesus testes

A substantial proportion of A_{dark} and A_{pale} spermatogonia in the adult rhesus testis shared a similar molecular phenotype with respect to the consensus stem cell markers tested. This observation raises questions about the distinct functional classification of A_{dark} and A_{pale} as reserve and renewing stem cells, respectively (Clermont, 1969; Clermont and Antar, 1973; Fouquet and Dadoune, 1986; van Alphen and de Rooij, 1986; Plant and Marshall, 2001; Ehmcke *et al*., 2005; Simorangkir *et al*., 2005). Perhaps, the dark and pale nuclear phenotypes correlate with stage of cell cycle (i.e. G0 versus G1/S/G2/M) rather than divergent stem cell functions. In addition, the molecular phenotypes of A_{pale} spermatogonia were more heterogeneous than A_{dark}. Most A_{dark} exhibit the phenotype GFRα1$^+$, PLZF$^+$, NGN3$^-$, cKIT$^-$. A_{pale} spermatogonia also exhibit this phenotype (GFRα1$^+$, PLZF$^+$, NGN3$^-$, cKIT$^-$) as well as the transition phenotypes (GFRα1$^+$, PLZF$^+$, NGN3$^+$, cKIT$^-$ and GFRα1$^+$, PLZF$^+$, NGN3$^+$, cKIT$^+$). It is also noteworthy that NGN3 expression encompasses the transition from cKIT$^-$ to cKIT$^+$ A_{pales} and therefore may coincide with a critical point in monkey spermatogenic differentiation. Future studies focused on this transition nexus in A_{pales} may identify regulatory networks associated with the initiation of spermatogonial differentiation in primates.

In summary, the conservation of spermatogonial molecular characteristics from rodents to monkeys provided insights into the identity of

putative rhesus SSCs. If our hypotheses about the rhesus SSC pool are correct, then important differences in the kinetics of SSC renewal and clonal expansion between rodents and primates may be inferred. Furthermore, our observations highlight the value of studying stem cells in higher mammals and the utility of cross-species comparisons. The molecular dissection of the rhesus spermatogenic lineage presented in this study provides a contemporary perspective for interpreting old and new experimental results and may help generate novel hypotheses about the biology and regenerative capacity of primate SSCs.

Supplementary data

Supplementary data are available at http://humrep.oxfordjournals.org/.

Acknowledgements

The authors thank Vivek Verma for helping to develop the xenotransplant assay, Drs Pier Paolo Pandolfi and Robin M. Hobbs for graciously providing the PLZF antibody for this study, and the staff of the Primate Core of the Pittsburgh SCCPIR and primate and rodent facilities of Magee-Womens Research Institute for maintaining the animals in this study. The authors would also like to acknowledge Lynda Guzik and Eric Lagasse for their help with FACS analyses.

Author contributions

B.P.H.: conception and design, collection and/or assembly of data, data analysis and interpretation, manuscript writing; M.S.: collection and/or assembly of data; D.R.S.: collection and/or assembly of data, data analysis and interpretation; T.C.: data analysis and interpretation; T.M.P.: conception and design, financial support, provision of study material, data analysis and interpretation, manuscript writing; K.E.O.: conception and design, financial support, administrative support, provision of study material, data analysis and interpretation, manuscript writing, final approval of manuscript.

Funding

This work was supported by the Eunice Kennedy Shriver National Institute of Child Health and Human Development (NICHD/NIH) through cooperative agreement U54 HD008610 as part of the Specialized Cooperative Centers Program in Reproduction and Infertility Research (SCCPIR), the Magee-Womens Research Institute and Foundation, NIH grants to K.E.O. (RR018500, AG024992, HD055475) and T.M.P. (HD013254), and an institutional NRSA postdoctoral fellowship (HD007332) to B.P.H.

References

Aponte PM, van Bragt MP, de Rooij DG, van Pelt AM. Spermatogonial stem cells: characteristics and experimental possibilities. *APMIS* 2005; **113**:727–742.

Baum CM, Weissman IL, Tsukamoto AS, Buckle AM, Peault B. Isolation of a candidate human hematopoietic stem-cell population. *Proc Natl Acad Sci USA* 1992;**89**:2804–2808.

Brinster RL. Male germline stem cells: from mice to men. *Science* 2007; **316**:404–405.

Brinster RL, Avarbock MR. Germline transmission of donor haplotype following spermatogonial transplantation. *Proc Natl Acad Sci USA* 1994; **91**:11303–11307.

Brinster RL, Zimmermann JW. Spermatogenesis following male germ-cell transplantation. *Proc Natl Acad Sci USA* 1994;**91**:11298–11302.

Brinster CJ, Ryu BY, Avarbock MR, Karagenc L, Brinster RL, Orwig KE. Restoration of fertility by germ cell transplantation requires effective recipient preparation. *Biol Reprod* 2003;**69**:412–420.

Buaas FW, Kirsh AL, Sharma M, McLean DJ, Morris JL, Griswold MD, de Rooij DG, Braun RE. Plzf is required in adult male germ cells for stem cell self-renewal. *Nat Genet* 2004;**36**:647–652.

Buageaw A, Sukhwani M, Ben-Yehudah A, Ehmcke J, Rawe VY, Pholpramool C, Orwig KE, Schlatt S. GDNF family receptor alpha1 phenotype of spermatogonial stem cells in immature mouse testes. *Biol Reprod* 2005;**73**:1011–1016.

Bucci LR, Meistrich ML. Effects of busulfan on murine spermatogenesis: cytotoxicity, sterility, sperm abnormalities, and dominant lethal mutations. *Mutat Res* 1987;**176**:259–268.

Cavicchia JC, Dym M. Ultrastructural characteristics of monkey spermatogonia and preleptotene spermatocytes. *Biol Reprod* 1978; **18**:219–228.

Clermont Y. Two classes of spermatogonial stem cells in the monkey (*Cercopithecus aethiops*). *Am J Anat* 1969;**126**:57–71.

Clermont Y. Kinetics of spermatogenesis in mammals: seminiferous epithelium cycle and spermatogonial renewal. *Physiol Rev* 1972; **52**:198–236.

Clermont Y, Antar M. Duration of the cycle of the seminiferous epithelium and the spermatogonial renewal in the monkey *Macaca arctoides*. *Am J Anat* 1973;**136**:153–165.

Clermont Y, Bustos-Obregon E. Re-examination of spermatogonial renewal in the rat by means of seminiferous tubules mounted 'in toto'. *Am J Anat* 1968;**122**:237–247.

Clermont Y, Leblond CP. Differentiation and renewal of spermatogonia in the monkey, *Macacus rhesus*. *Am J Anat* 1959;**104**:237–271.

Costoya JA, Hobbs RM, Barna M, Cattoretti G, Manova K, Sukhwani M, Orwig KE, Wolgemuth DJ, Pandolfi PP. Essential role of Plzf in maintenance of spermatogonial stem cells. *Nat Genet* 2004;**36**:653–659.

de Rooij DG, Russell LD. All you wanted to know about spermatogonia but were afraid to ask. *J Androl* 2000;**21**:776–798.

Dobrinski I, Ogawa T, Avarbock MR, Brinster RL. Computer assisted image analysis to assess colonization of recipient seminiferous tubules by spermatogonial stem cells from transgenic donor mice. *Mol Reprod Dev* 1999;**53**:142–148.

Dym M, Jia MC, Dirami G, Price JM, Rabin SJ, Mocchetti I, Ravindranath N. Expression of c-kit receptor and its autophosphorylation in immature rat type A spermatogonia. *Biol Reprod* 1995;**52**:8–19.

Ehmcke J, Luetjens CM, Schlatt S. Clonal organization of proliferating spermatogonial stem cells in adult males of two species of non-human primates, *Macaca mulatta* and *Callithrix jacchus*. *Biol Reprod* 2005; **72**:293–300.

Falciatori I, Borsellino G, Haliassos N, Boitani C, Corallini S, Battistini L, Bernardi G, Stefanini M, Vicini E. Identification and enrichment of spermatogonial stem cells displaying side-population phenotype in immature mouse testis. *FASEB J* 2004;**18**:376–378.

Fouquet JP, Dadoune JP. Renewal of spermatogonia in the monkey (*Macaca fascicularis*). *Biol Reprod* 1986;**35**:199–207.

Fujita K, Ohta H, Tsujimura A, Takao T, Miyagawa Y, Takada S, Matsumiya K, Wakayama T, Okuyama A. Transplantation of spermatogonial stem cells isolated from leukemic mice restores fertility without inducing leukemia. *J Clin Invest* 2005;**115**:1855–1861.

Gaskell TL, Esnal A, Robinson LL, Anderson RA, Saunders PT. Immunohistochemical profiling of germ cells within the human fetal testis: identification of three subpopulations. *Biol Reprod* 2004; **71**:2012–2021.

Geens M, Goossens E, De BG, Ning L, Van SD, Tournaye H. Autologous spermatogonial stem cell transplantation in man: current obstacles for a future clinical application. *Hum Reprod Update* 2008; **14**:121–130.

Goldschneider I, Gordon LK, Morris RJ. Demonstration of Thy-1 antigen on pluripotent hemopoietic stem cells in the rat. *J Exp Med* 1978; **148**:1351–1366.

Greenbaum MP, Yan W, Wu MH, Lin YN, Agno JE, Sharma M, Braun RE, Rajkovic A, Matzuk MM. TEX14 is essential for intercellular bridges and fertility in male mice. *Proc Natl Acad Sci USA* 2006;**103**:4982–4987.

Gupta G, Maikhuri JP, Setty BS, Dhar JD. Seasonal variations in daily sperm production rate of rhesus and bonnet monkeys. *J Med Primatol* 2000; **29**:411–414.

Hermann BP, Sukhwani M, Lin CC, Sheng Y, Tomko J, Rodriguez M, Shuttleworth JJ, McFarland D, Hobbs RM, Pandolfi PP *et al*. Characterization, cryopreservation and ablation of spermatogonial stem cells in adult rhesus macaques. *Stem Cells* 2007;**25**:2330–2338.

Honaramooz A, Behboodi E, Megee SO, Overton SA, Galantino-Homer H, Echelard Y, Dobrinski I. Fertility and germline transmission of donor haplotype following germ cell transplantation in immunocompetent goats. *Biol Reprod* 2003;**69**:1260–1264.

Kanatsu-Shinohara M, Toyokuni S, Shinohara T. CD9 is a surface marker on mouse and rat male germline stem cells. *Biol Reprod* 2004;**70**:70–75.

Kim Y, Turner D, Nelson J, Dobrinski I, McEntee M, Travis A. Production of donor-derived sperm after spermatogonial stem cell transplantation in the dog. *Reproduction* 2008;**136**:823–831.

Kubota H, Avarbock MR, Brinster RL. Spermatogonial stem cells share some, but not all, phenotypic and functional characteristics with other stem cells. *Proc Natl Acad Sci USA* 2003;**100**:6487–6492.

Lassalle B, Bastos H, Louis JP, Riou L, Testart J, Dutrillaux B, Fouchet P, Allemand I. 'Side population' cells in adult mouse testis express Bcrp1 gene and are enriched in spermatogonia and germinal stem cells. *Development* 2004;**131**:479–487.

Lo KC, Brugh VM III, Parker M, Lamb DJ. Isolation and enrichment of murine spermatogonial stem cells using rhodamine 123 mitochondrial dye. *Biol Reprod* 2005;**72**:767–771.

Manova K, Nocka K, Besmer P, Bachvarova RF. Gonadal expression of c-kit encoded at the W locus of the mouse. *Development* 1990; **110**:1057–1069.

Marshall GR, Plant TM. Puberty occurring either spontaneously or induced precociously in rhesus monkey (*Macaca mulatta*) is associated with a marked proliferation of Sertoli cells. *Biol Reprod* 1996;**54**:1192–1199.

Meng X, Lindahl M, Hyvonen ME, Parvinen M, de Rooij DG, Hess MW, Raatikainen-Ahokas A, Sainio K, Rauvala H, Lakso M *et al*. Regulation of cell fate decision of undifferentiated spermatogonia by GDNF. *Science* 2000;**287**:1489–1493.

Muller T, Eildermann K, Dhir R, Schlatt S, Behr R. Glycan stem-cell markers are specifically expressed by spermatogonia in the adult non-human primate testis. *Hum Reprod* 2008;**23**:2292–2298.

Nagano MC. Homing efficiency and proliferation kinetics of male germ line stem cells following transplantation in mice. *Biol Reprod* 2003; **69**:701–707.

Nagano M, Brinster RL. Spermatogonial transplantation and reconstitution of donor cell spermatogenesis in recipient mice. *APMIS* 1998; **106**:47–57.

Nagano M, Avarbock MR, Brinster RL. Pattern and kinetics of mouse donor spermatogonial stem cell colonization in recipient testes. *Biol Reprod* 1999;**60**:1429–1436.

Nagano M, Brinster CJ, Orwig KE, Ryu BY, Avarbock MR, Brinster RL. Transgenic mice produced by retroviral transduction of male germ-line stem cells. *Proc Natl Acad Sci USA* 2001;**98**:13090–13095.

Nakagawa T, Nabeshima Y, Yoshida S. Functional identification of the actual and potential stem cell compartments in mouse spermatogenesis. *Dev Cell* 2007;**12**:195–206.

Ogawa T, Aréchaga JM, Avarbock MR, Brinster RL. Transplantation of testis germinal cells into mouse seminiferous tubules. *Int J Dev Biol* 1997;**41**:111–122.

Ogawa T, Dobrinski I, Avarbock MR, Brinster RL. Transplantation of male germ line stem cells restores fertility in infertile mice. *Nat Med* 2000; **6**:29–34.

Orwig KE, Schlatt S. Cryopreservation and transplantation of spermatogonia and testicular tissue for preservation of male fertility. *J Natl Cancer Inst Monogr* 2005;**34**:51–56.

Orwig KE, Shinohara T, Avarbock MR, Brinster RL. Functional analysis of stem cells in the adult rat testis. *Biol Reprod* 2002;**66**:944–949.

Plant TM, Marshall GR. The functional significance of FSH in spermatogenesis and the control of its secretion in male primates. *Endocr Rev* 2001;**22**:764–786.

Plant TM, Ramaswamy S, Simorangkir D, Marshall GR. Postnatal and pubertal development of the rhesus monkey (*Macaca mulatta*) testis. *Ann NY Acad Sci* 2005;**1061**:149–162.

Ramaswamy S, Marshall GR, McNeilly AS, Plant TM. Dynamics of the follicle-stimulating hormone (FSH)-inhibin B feedback loop and its role in regulating spermatogenesis in the adult male rhesus monkey (*Macaca mulatta*) as revealed by unilateral orchidectomy. *Endocrinology* 2000a;**141**:18–27.

Ramaswamy S, Plant TM, Marshall GR. Pulsatile stimulation with recombinant single chain human luteinizing hormone elicits precocious sertoli cell proliferation in the juvenile male rhesus monkey (*Macaca mulatta*). *Biol Reprod* 2000b;**63**:82–88.

Ryu BY, Orwig KE, Avarbock MR, Brinster RL. Stem cell and niche development in the postnatal rat testis. *Dev Biol* 2003;**263**: 253–263.

Ryu BY, Orwig KE, Kubota H, Avarbock MR, Brinster RL. Phenotypic and functional characteristics of spermatogonial stem cells in rats. *Dev Biol* 2004;**274**:158–170.

Ryu BY, Kubota H, Avarbock MR, Brinster RL. Conservation of spermatogonial stem cell self-renewal signaling between mouse and rat. *Proc Natl Acad Sci USA* 2005;**102**:14302–14307.

Schlesser HN, Simon L, Hofmann MC, Murphy KM, Murphy T, Hess RA, Cooke PS. Effects of ETV5 (ets variant gene 5) on testis and body growth, time course of spermatogonial stem cell loss, and fertility in mice. *Biol Reprod* 2008;**78**:483–489.

Schrans-Stassen BH, van de Kant HJ, de Rooij DG, van Pelt AM. Differential expression of c-kit in mouse undifferentiated and differentiating type A spermatogonia. *Endocrinology* 1999;**140**:5894–5900.

Sharpe RM. Regulation of spermatogenesis. In: Knobil E, Neill JD (eds), *The Physiology of Reproduction*. New York: Raven Press, Ltd, 1994, 1363–1434.

Shinohara T, Avarbock MR, Brinster RL. β1- and α6-integrin are surface markers on mouse spermatogonial stem cells. *Proc Natl Acad Sci USA* 1999;**96**:5504–5509.

Shinohara T, Orwig KE, Avarbock MR, Brinster RL. Spermatogonial stem cell enrichment by multiparameter selection of mouse testis cells. *Proc Natl Acad Sci USA* 2000;**97**:8346–8351.

Simorangkir DR, Marshall GR, Plant TM. Sertoli cell proliferation during prepubertal development in the rhesus monkey (*Macaca mulatta*) is maximal during infancy when gonadotropin secretion is robust. *J Clin Endocrinol Metab* 2003;**88**:4984–4989.

Simorangkir DR, Marshall GR, Ehmcke J, Schlatt S, Plant TM. Prepubertal expansion of dark and pale type A spermatogonia in the rhesus monkey

(*Macaca mulatta*) results from proliferation during infantile and juvenile development in a relatively gonadotropin independent manner. *Biol Reprod* 2005;**73**:1109–1115.

Sorrentino V, Giorgi M, Geremia R, Besmer P, Rossi P. Expression of the c-kit proto-oncogene in the murine male germ cells. *Oncogene* 1991; **6**:149–151.

Spangrude GJ, Heimfeld S, Weissman IL. Purification and characterization of mouse hematopoietic stem cells. *Science* 1988;**241**:58–62.

Tajima Y, Sawada K, Morimoto T, Nishimune Y. Switching of mouse spermatogonial proliferation from the c-kit receptor-independent type to the receptor-dependent type during differentiation. *J Reprod Fertil* 1994;**102**:117–122.

Tegelenbosch RAJ, de Rooij DG. A quantitative study of spermatogonial multiplication and stem cell renewal in the C3H/101 F1 hybrid mouse. *Mutat Res* 1993;**290**:193–200.

Thayer KA, Ruhlen RL, Howdeshell KL, Buchanan DL, Cooke PS, Preziosi D, Welshons WV, Haseman J, vom Saal FS. Altered prostate growth and daily sperm production in male mice exposed prenatally to subclinical doses of 17alpha-ethinyl oestradiol. *Hum Reprod* 2001; **16**:988–996.

Tokuda M, Kadokawa Y, Kurahashi H, Marunouchi T. CDH1 is a specific marker for undifferentiated spermatogonia in mouse testes. *Biol Reprod* 2007;**76**:130–141.

van Alphen MM, de Rooij DG. Depletion of the seminiferous epithelium of the rhesus monkey, *Macaca mulatta*, after X-irradiation. *Br J Cancer Suppl* 1986;**7**:102–104.

van Bragt MP, Roepers-Gajadien HL, Korver CM, Bogerd J, Okuda A, Eggen BJ, de Rooij DG, van Pelt AM. Expression of the pluripotency marker UTF1 is restricted to a subpopulation of early A spermatogonia in rat testis. *Reproduction* 2008;**136**:33–40.

Yoshida S, Nabeshima Y, Nakagawa T. Stem cell heterogeneity: actual and potential stem cell compartments in mouse spermatogenesis. *Ann NY Acad Sci* 2007a;**1120**:47–58.

Yoshida S, Takakura A, Ohbo K, Abe K, Wakabayashi J, Yamamoto M, Suda T, Nabeshima Yi. Neurogenin3 delineates the earliest stages of spermatogenesis in the mouse testis. *Dev Biol* 2004;**269**:447–458.

Yoshida S, Sukeno M, Nabeshima Y. A vasculature-associated niche for undifferentiated spermatogonia in the mouse testis. *Science* 2007b; **317**:1722–1726.

Yoshinaga K, Nishikawa S, Ogawa M, Hayashi S, Kunisada T, Fujimoto T, Nishikawa S. Role of c-kit in mouse spermatogenesis: identification of spermatogonia as a specific site of c-kit expression and function. *Development* 1991;**113**:689–699.

Submitted on January 15, 2009; resubmitted on February 28, 2009; accepted on March 3, 2009